RJC

RASĀYAN *J. Chem.*
Vol. 18 | No. 3 |1488-1494| July-September | 2025
ISSN: 0974-1496 | e-ISSN: 0976-0083 | CODEN: RJCABP
http://www.rasayanjournal.com
http://www.rasayanjournal.co.in

VIOLAXANTHIN FROM *Graptophyllum pictum*: POTENT ANTI-INFLAMMATORY AND ANTIOXIDANT ACTIVITY REVEALED THROUGH MOLECULAR DOCKING AND BIOAVAILABILITY STUDY

F. A. Makkiyah[1], E. P. Rahmi[1], D.L.C. Pradana[1], F. R. Mahendra[2], G. M. Gholam[2], R. Kartiman[3] and W. Nurcholis[2,4,✉]

[1]Faculty of Medicine, Universitas Pembangunan Nasional Veteran, Jakarta, Indonesia
[2]Department of Biochemistry, IPB University, West Java, Indonesia
[3]Research Center for Applied Botany, Research Organization for Life Science and Environment, National Research and Innovation Agency-Indonesia (BRIN), West Java, Indonesia.
[4]Tropical Biopharmaca Research Center, IPB University, West Java, Indonesia
✉Corresponding author: wnurcholis@apps.ipb.ac.id

ABSTRACT

Graptophyllum pictum (L.) Griff., commonly known as "daun ungu or daun wungu," is a medicinal plant renowned for its diverse pharmacological properties, contributing significantly to SDG 3: Good Health and Well-being. This study explores the therapeutic potential of its secondary metabolites through molecular docking, bioavailability assessment, and density functional theory (DFT) analysis, specifically targeting anti-inflammatory pathways associated with chronic diseases. Violaxanthin, a key compound, exhibited strong binding affinities with inflammatory and oxidative stress-related proteins such as interleukin-1 alpha (IL-1α) and tumor necrosis factor-alpha (TNF-α), with binding energies reaching -10.2 kcal/mol. Bioavailability studies revealed high absorption rates for violaxanthin (91.43%) despite minor violations of Lipinski's Rule of Five. Membrane permeability analysis demonstrated favorable energy profiles, highlighting violaxanthin's potential for effective cellular uptake. Furthermore, DFT calculations indicated excellent electronic stability with a narrow HOMO-LUMO energy gap of -0.0836 eV. These findings support the role of *G. pictum* metabolites, particularly violaxanthin, as promising candidates for anti-inflammatory and antioxidant drug development, suggesting their potential in addressing treatment gaps in inflammatory diseases. Further in vivo studies are recommended to validate these computational predictions and assess long-term safety. This research contributes to sustainable therapeutic development aligned with the SDG 3 goals.

Keywords: *Graptophyllum pictum*, Molecular docking, Violaxanthin, Bioavailability, DFT analysis, Anti-inflammatory.

RASĀYAN *J. Chem.*, Vol. 18, No. 3, 2025

INTRODUCTION

The escalating prevalence of chronic diseases such as diabetes, cancer, and inflammatory disorders underscores the urgent need for novel therapeutic agents. According to recent WHO reports, chronic inflammatory diseases affect millions globally, emphasizing the critical need for safe and effective therapies (WHO, 2023).[1] While synthetic drugs remain pivotal, their associated side effects and resistance profiles have shifted focus toward natural products. Plants have long served as a rich reservoir of bioactive compounds, offering a spectrum of pharmacological benefits. Among these, *Graptophyllum pictum*, locally referred to as "daun ungu or daun wungu" in Indonesia, stands out due to its remarkable phytochemical diversity and therapeutic potential. The exploration of plants with traditional anti-inflammatory uses has gained momentum, as shown by the development of formulations based on Ipomoea batatas for inflammation control.[2] *G. pictum* is an indigenous medicinal plant traditionally employed to treat a range of ailments, from inflammation to hemorrhoids. Recent phytochemical investigations have identified an array of bioactive constituents in *G. pictum*, including flavonoids, steroids, glycosides, tannins, saponins, chlorophyll, non-toxic alkaloids, and anthocyanins.[3,4] These compounds not only underpin its efficacy in traditional medicine but also highlight its potential for modern pharmaceutical development. Despite the

http://doi.org/10.31788/RJC.2025.1839258

well-documented pharmacological activities of *G. pictum*, including its antimicrobial, antioxidant, anti-inflammatory, anti-diabetic, and wound-healing properties,[5-6] critical questions remain unanswered. The molecular basis underlying these activities, particularly ligand-receptor interactions and their implications for drug design, has yet to be fully elucidated. Additionally, while studies have demonstrated the safety of *G. pictum* extracts,[7] detailed evaluations of its bioavailability and permeability across biological membranes are limited. These gaps hinder the plant's progression from traditional use to scientifically validated pharmaceutical applications. This study aims to bridge the existing knowledge gaps by leveraging advanced computational techniques to investigate the pharmacological potential of *G. pictum*. Specifically, the study focuses on molecular docking and dynamics simulations, bioavailability assessment, and density functional theory (DFT) analysis to: (1) Identify key bioactive compounds in *G. pictum* responsible for its therapeutic activities; (2) Elucidate ligand-receptor interactions at the molecular level; and (3) Evaluate bioavailability, permeability, and safety profiles of the compounds. By integrating in silico and experimental findings, this research seeks to validate the therapeutic potential of *G. pictum*, paving the way for its incorporation into modern phytomedicine, thereby directly contributing to achieving SDG 3: Good Health and Well-being.

EXPERIMENTAL

Materials

Protein structures were retrieved from the Research Collaboratory for Structural Bioinformatics (RCSB) Protein Data Bank (PDB) in *.pdb format. Selection criteria included crystal resolution (<3.0 Å), presence of co-crystallized ligands, and accurate ligand positioning within binding pockets.[8,9] Ligands corresponding to secondary metabolites of *G. pictum* were obtained from the literature or designed using MarvinSketch. PubChem was utilized for downloading ligand data in *.sdf format, followed by optimization using the MMFF94 force field.[10] Computational tools, such as PyMol2, AutoDock Vina, and ORCA, were employed for docking simulations and density functional theory (DFT) analysis.

Receptor Preparation

Proteins were validated using Ramachandran plots from PDBsum to ensure geometric integrity. Preparation steps involved the addition of missing hydrogens, atoms, and residues using pdbfixer workflow.[11] Non-essential chains, ligands, and water molecules were removed using PyMol2. The processed protein structures were converted to *.pdbqt format by assigning charges and protons using AutoDock Tools.

Ligand Preparation

Secondary metabolites, including flavonoids, steroids, and anthocyanins from *G. pictum*, were either downloaded from PubChem or drawn de novo. These ligands were energy-minimized using the MMFF94 force field and saved in *.pdbqt format via Open Babel and PyMol2 commands. Ligands were archived in a *.zip format for subsequent virtual screening.

Molecular Docking and Gridbox Validation

Docking simulations were conducted using AutoDock Vina integrated with Google Collaboratory. Validation of docking protocols involved redocking co-crystallized ligands to confirm binding poses with root-mean-square deviation (RMSD) values below 2.0 Å.[12] Gridbox dimensions were determined by aligning with the active site of each receptor, using a range of 2 Å increments to evaluate binding site coverage. The results were expressed as binding affinity values (kcal/mol).

Virtual Screening

The virtual screening employed the AutoDock Vina algorithm, using optimized receptor and ligand files as input. Binding affinities were calculated, and ligand-receptor complexes were ranked based on energy scores. The top candidates were subjected to Molecular Mechanics/Generalized Born Surface Area (MM/GBSA) rescoring to refine binding energy predictions.[13]

Bioavailability and Permeability Analysis

The pkCSM web server was used to predict the pharmacokinetic properties of ligands, including Lipinski's Rule of Five parameters, Caco-2 permeability, and human intestinal absorption rates.[14] Permeability through biological membranes was further analyzed using PerMM, which calculates energy profiles and membrane-binding affinities using the DOPC bilayer model.[15]

DFT Analysis

Density functional theory (DFT) calculations were performed using ORCA with the B3LYP functional. Ligands were optimized for energy parameters in Avogadro and prepared for analysis in ORCA format. HOMO, LUMO, and energy gap calculations were carried out to assess molecular stability and electron-donating/withdrawing capabilities.[16]

Visualization of Interactions

Two-dimensional interactions were visualized using Discovery Studio, focusing on hydrogen bonding, electrostatic interactions, and van der Waals forces. Three-dimensional interactions and binding pocket analyses were performed in PyMol2, highlighting active and catalytic site interactions for ligand-receptor complexes.

Statistical Analysis

Binding affinities and other quantitative metrics were analyzed using descriptive statistics. Comparative assessments were conducted with literature values to validate results and ensure reliability.[17]

RESULTS AND DISCUSSION

Docking Results and Validation

The docking simulations revealed significant binding affinities between the secondary metabolites of *G. pictum* and key protein targets. Violaxanthin exhibited the strongest binding affinity with interleukin-1 alpha (IL-1α), achieving a binding energy of -10.2 kcal/mol in a gridbox size of 40×40×40, with an RMSD value of 0.62 Å (Table-1). This RMSD value indicates a highly reliable docking conformation. Similarly, anacardic acid and schaftoside demonstrated favorable interactions with inducible nitric oxide synthase (iNOS) and tumor necrosis factor-alpha (TNF-α), respectively. These outcomes align with previous studies underscoring the importance of gridbox validation in achieving precise docking results.[18]

Table-1: Grid box Coordination and Validation

Receptor (PDB-ID)	Coordinates (x,y,z)	Gridbox Size	RMSD (Å)	Binding Affinity (kcal/mol)
Interleukin-1 alpha (8C3U)	-18.22; -4.82; -41.95	gridbox_x40_y40_z40	0.62	-10.2
		gridbox_x50_y50_z50	0.82	-10.0
		gridbox_x30_y30_z30	0.87	-10.0
		gridbox_x20_y20_z20	0.88	-10.0
		gridbox_x10_y10_z10	0.98	-7.5
Myeloperoxide (4C1M)	18.14; -19.24; -2.60	gridbox_x30_y30_z30	2.01	-9.3
		gridbox_x40_y40_z40	2.22	-9.2
		gridbox_x50_y50_z50	2.29	-9.1
		gridbox_x20_y20_z20	2.29	-9.5
		gridbox_x10_y10_z10	3.03	-8.2
N-methyl-D-aspartate receptor (5EWM)	81.00; 5.90; -32.42	gridbox_x40_y40_z40	1.59	-10.6
		gridbox_x50_y50_z50	2.00	-10.5
		gridbox_x10_y10_z10	2.71	-10.3
		gridbox_x20_y20_z20	3.28	-10.5
		gridbox_x30_y30_z30	3.52	-10.6
Inducible nitric oxide synthase (3E7G)	37.11; 35.04; 32.02	gridbox_x40_y40_z40	0.29	-8.5
		gridbox_x20_y20_z20	0.30	-8.5
		gridbox_x50_y50_z50	0.31	-8.5
		gridbox_x30_y30_z30	0.34	-8.5
		gridbox_x10_y10_z10	0.34	-8.4
Tumor necrosis factor (2AZ5)	-8.33; 68.22; 19.96	gridbox_x50_y50_z50	2.48	-9.9
		gridbox_x30_y30_z30	2.76	-10.1
		gridbox_x10_y10_z10	2.63	-9.7
		gridbox_x20_y20_z20	2.65	-10.1
		gridbox_x50_y50_z50	2.48	-9.9

Ligand-Receptor Interaction Analysis

The molecular interactions of violaxanthin were notably robust, particularly with IL-1α. Violaxanthin formed hydrogen bonds with key residues Lys92 and Val47, while van der Waals interactions provided additional stability (Fig.-1). These interactions were superior to those of the co-crystal ligand T9C, which engaged fewer active-site residues and displayed weaker binding stability.

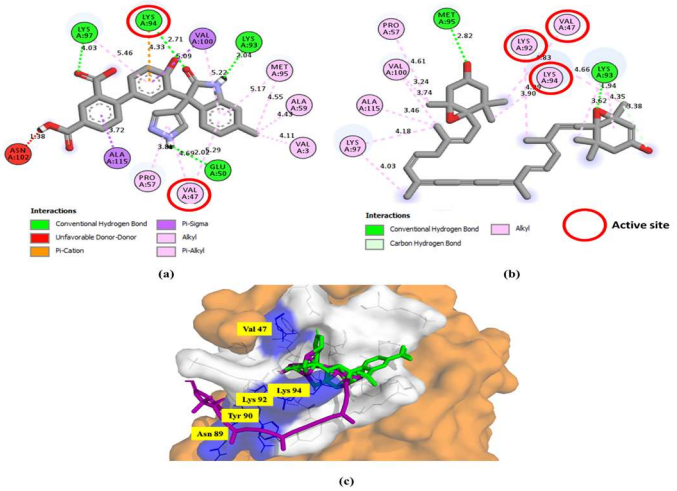

Fig.-1: Two-Dimensional Interaction Between IL-1α Receptor and Ligands: (a) Co-crystal Ligand T9C; (b) Test Ligand Violaxanthin. Three-Dimensional Interaction (c) Between the Active (White Surface) and Catalytic (Blue Surface) Sides of TNF-Alpha Receptor Towards the Co-Crystal Ligand (Green Stick) and the Test Ligand Violaxanthin (Purple Stick).

In the case of TNF-α, violaxanthin exhibited extensive van der Waals interactions with active residues Leu57 and Tyr119 (Fig.-2). Unlike the comparator ligand SPD304, violaxanthin formed additional hydrogen and alkyl interactions, enhancing its binding potential. These observations highlight the unique interaction profile of violaxanthin compared to known inhibitors, offering insights into its potent anti-inflammatory mechanisms.

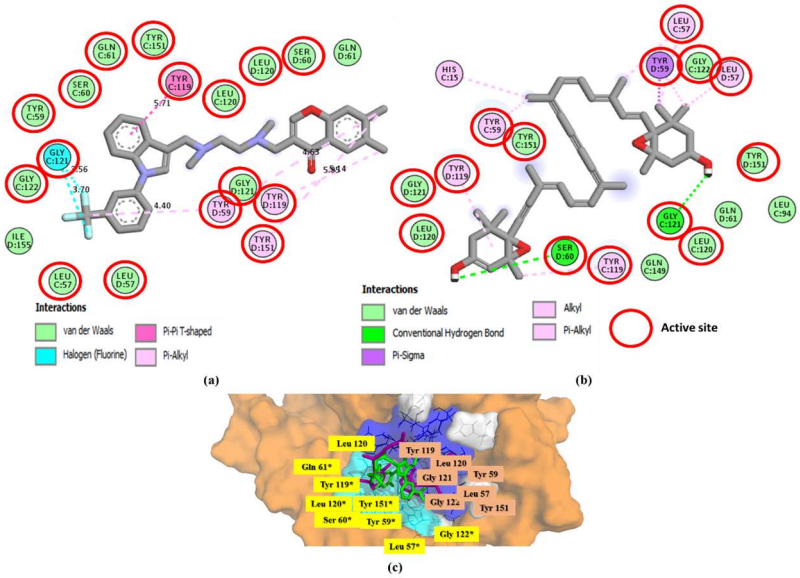

Fig.-2: Two-Dimensional Interaction Between TNF-Alpha Receptor and (a) SPD304 (co-crystal ligand), (b) Violaxanthin. Three-Dimensional Interaction (c) Between the Active (White Surface) and Catalytic (Blue Surface) Sides of TNF-Alpha Receptor Towards the Co-Crystal Ligand (Green Stick) and the Test Ligand Violaxanthin (Purple Stick)

Bioavailability Assessment

The pharmacokinetic evaluation of *G. pictum*'s metabolites revealed favorable bioavailability profiles, with violaxanthin showing an intestinal absorption rate of 91.43% (Table-2). Despite minor violations of Lipinski's Rule of Five, such as molecular weight and LogP exceeding optimal thresholds, violaxanthin exhibited strong permeability characteristics (Table-3). Anacardic acid and 12-oxo-phytodienoic acid also displayed desirable bioavailability metrics, supporting their suitability as drug candidates.

Table-2: Bioavailability Parameters of *G. pictum* Metabolites

Compounds	Caco2 permeability	Intestinal absorption (human) (%)	P-glycoprotein substrate
Violaxanthin	1.12	91.43	Yes
Anarcardic acid	1.21	88.14	Yes
12-Oxo-phytodienoic acid	1.47	94.30	Yes
Xanthohumol	1.02	89.39	Yes
Haplophytin	1.30	96.64	Yes
Corymboside	-0.64	30.63	Yes
Schaftoside	-0.64	30.63	Yes

*Red numbers indicate that the parameter is not proper.

Table-3: Physicochemical Parameters

Compounds	MW	LogP	SA	RotB	H-bond	
					Acceptors	Donors
Violaxanthin	600.88	8.97	266.56	10	4	2
Anarcardic acid	348.53	6.72	153.02	15	2	2
12-Oxo-phytodienoic acid	292.42	4.53	127.68	11	2	1
Xanthohumol	354.40	4.22	152.02	6	5	3
Haplophytin	257.29	2.72	110.22	1	3	1
Corymboside	564.50	-1.75	224.31	4	14	10
Schaftoside	564.50	-1.75	224.31	4	14	10

*Red numbers indicate parameters that violate the Lipinski rule of five.

Membrane Permeability Analysis

The permeability profiles, as predicted by PerMM, indicated that violaxanthin and anacardic acid exhibited strong passive transport across the lipid bilayer. Energy distribution analyses (Fig.-3) revealed consistent negative energy profiles for violaxanthin during membrane translocation, signifying favorable interactions with the lipid environment. Conformational flexibility during bilayer crossing further enhanced violaxanthin's efficiency, as shown in Fig.-4. Figure-3 shows the energy profiles of violaxanthin and other metabolites during membrane permeability studies. These profiles align with prior findings linking hydrophobicity and molecular adaptability to enhanced permeability.[15]

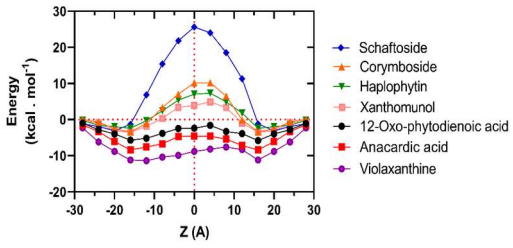

Fig.-3: Energy Distribution of Violaxanthin and other Ligands During Membrane Permeability Analysis

DFT Results

The DFT analysis of violaxanthin provided insights into its electronic stability and reactivity. The calculated HOMO and LUMO energies of -0.1703 eV and -0.0867 eV, respectively, resulted in an energy gap of -0.0836 eV. This narrow gap indicates a propensity for electron transfer, enhancing ligand-receptor interactions (Fig.-5). Figure-5 visualizes the HOMO-LUMO orbitals of violaxanthin, highlighting its suitability for stabilizing molecular interactions. These properties, combined with favorable docking results, emphasize its role as a promising candidate for therapeutic development.

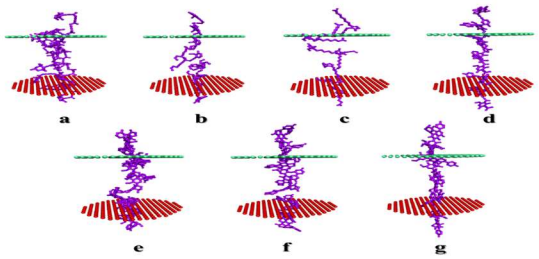

Fig.-4: Conformational Changes of Violaxanthin and other Ligands During Membrane Transport. (a) Violaxanthin, (b) Anacardic Acid, (c) Asam 12-oxo-fitodienoat, (d) Xanthohumol, (e) Haplofitin, (f) Corymboside, (g) Schaftosid

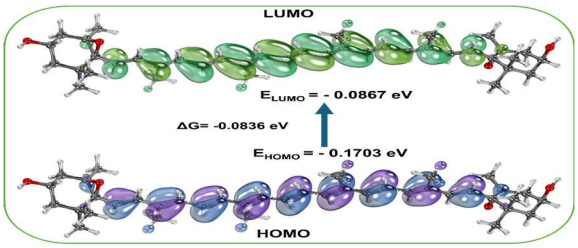

Fig.-5: HOMO-LUMO Visualization of Violaxanthin from DFT Calculations

Our findings support the notion that violaxanthin is a promising candidate for anti-inflammatory therapy. Its high binding affinity and bioavailability reinforce its pharmacological potential. These insights align with previous studies on polyherbal formulations that integrate multiple antioxidant-rich ingredients for enhanced efficacy.[19] The stability and permeability of violaxanthin through membranes further confirm its potential, consistent with other studies demonstrating effective transdermal or mucosal formulations of herbal compounds.[20]

CONCLUSION

This study highlights the therapeutic potential of secondary metabolites from *G. pictum*, focusing on their interactions with key protein targets associated with inflammation and oxidative stress. Molecular docking results identified violaxanthin as a lead compound, exhibiting strong binding affinities and robust interactions with target receptors. Bioavailability and permeability analyses further validated violaxanthin's pharmacokinetic suitability, with high intestinal absorption and efficient passive transport across biological membranes. Additionally, DFT calculations revealed electronic properties conducive to stable and reactive interactions with protein targets. These findings underscore the value of *G. pictum* as a source of natural compounds for drug discovery, particularly for anti-inflammatory and antioxidant therapies. Violaxanthin demonstrated superior performance compared to synthetic reference ligands, reinforcing its potential as a lead candidate. This study directly supports SDG 3: Good Health and Well-being by contributing to the development of safe and effective therapeutic alternatives derived from natural sources. However, further experimental validation, including in vivo studies and detailed toxicological assessments, is essential to confirm its efficacy and safety. This integrative approach, combining computational and pharmacokinetic evaluations, provides a foundation for advancing *G. pictum* into modern phytomedicine applications.

ACKNOWLEDGMENTS

The authors express their heartfelt gratitude to the Faculty of Medicine, Universitas Pembangunan Nasional Veteran Jakarta, Indonesia, for their significant support and contributions that greatly facilitated this research.

CONFLICT OF INTERESTS

The authors declare that there is no conflict of interest.

AUTHOR CONTRIBUTIONS

The present work is related to *SDG-3: Good Health and Well-being*. All the authors contributed significantly to this manuscript, participated in reviewing/editing and approved the final draft for publication. The research profile of the authors can be verified from their ORCID ids, given below:

Feda Anisah Makkiyah https://orcid.org/0000-0001-6697-8069

Eldiza Puji Rahmi https://orcid.org/0000-0002-0385-9246
Dhigna Luthfiyani Citra Pradana https://orcid.org/0000-0001-5873-3539
Fachrur Rizal Mahendra https://orcid.org/0009-0003-9312-0027
Gusnia Meilin Gholam https://orcid.org/0000-0001-7142-5856
Roni Kartiman https://orcid.org/0009-0008-5140-1337
Waras Nurcholis https://orcid.org/0000-0001-7047-5093

REFERENCES

1. World Health Organization (WHO), Global Health Estimates: Chronic Diseases and Conditions, WHO Press, Geneva, Switzerland (2023). https://www.who.int/data/global-health-estimates
2. O. Pramiastuti, M.I. Rizqi, L.G. Nurhidayati, and G.R. Firsty, *Jurnal Jamu Indonesia*, **10**, 110(2025), https://doi.org/10.56108/jji.v10i2.402
3. F. Makkiyah, E.P. Rahmi, R. Revina, T. Susantiningsih, and Y. Setyaningsih, *Pharmacognosy Journal*, **13**, 835(2021), https://doi.org/10.5530/pj.2021.13.106
4. J.A. Priyanto, M.E. Prastya, M. Minarti, and V. Permatasari, *Turkish Journal of Pharmaceutical Sciences*, **21**, 133(2024), https://doi.org/10.4274/tjps.galenos.2023.95690
5. I. Diyatri, T. Kusumaningsih, Tantiana, and A.R. Hidayanto, *Malaysian Journal of Medicine and Health Sciences*, **16**, 92(2020).
6. F.A. Makkiyah, E.P. Rahmi, T. Susantiningsih, N. Marliani, R.A. Arista, and W. Nurcholis, *Journal of Applied Pharmaceutical Science*, **13**, 214(2023), https://doi.org/10.7324/JAPS.2023.117043
7. I. Kusumawati, S. Rullyansyah, M.F. Warsito, M. Zdulqornain, F. Nuraini, A.F. Rizka, Y.A. Pratama, R. Widyowati, E.P. Hestianah, and K. Matsunami, *Farmacia*, **71**, 72(2023), https://doi.org/10.31925/farmacia.2023.1.10
8. L. Heo and M. Feig, *BioRxiv* (2023), https://doi.org/10.1101/2023.05.22.541652
9. W. Zhung, H. Kim, and W.Y. Kim, *Nature Communications*, **15**, 2688(2024), https://doi.org/10.1038/s41467-024-47011-2
10. V.O. Samarskaya, A.V. Kovalenko, G.A. Sroslova, M.V. Postnova, A.A. Shiroky, and A.G. Serov, *Proceedings of SPIE*, **11067**, 176(2019).
11. M. W. Chang, C. Ayeni, S. Breuer, and B. E. Torbett, *PLoS One*, **5**, e11955(2010), https://doi.org/10.1371/journal.pone.0011955
12. H. Rangwala and G. Karypis, *Proteins: Structure, Function, and Bioinformatics*, **72**, 1005(2008), https://doi.org/10.1002/prot.21998
13. M. Yang, Z. Bo, T. Xu, B. Xu, D. Wang, and H. Zheng, *Briefings in Bioinformatics*, **24**, bbad218 (2023), https://doi.org/10.1093/bib/bbad218
14. D.E.V. Pires, T.L. Blundell, and D.B. Ascher, *Journal of Medicinal Chemistry*, **58**, 4066(2015), https://doi.org/10.1021/acs.jmedchem.5b00104
15. A.L. Lomize, J.M. Hage, K. Schnitzer, K. Golobokov, M.B. LaFaive, A.C. Forsyth, and I.D. Pogozheva, *Journal of Chemical Information and Modeling*, **59**, 3094(2019), https://doi.org/10.1021/acs.jcim.9b00225
16. K.E. Anwer, Z.K. Hamza, and R.M. Ramadan, *Scientific Reports*, **13**, 15598(2023), https://doi.org/10.1038/s41598-023-42714-w
17. W.Y. Kim, W. Zhung, and H. Kim, *Nature Communications*, **15**, 2688(2023), https://doi.org/10.21203/rs.3.rs-3388359/v1
18. F. Flachsenberg, C. Ehrt, T. Gutermuth, and M. Rarey, *Zenodo, Version v1* (2023), https://doi.org/10.5281/zenodo.7579502
19. T.K. Wardani, E. Arianingsih, A. Syarifah, A. Hamad, and D. Hartanti, *Jurnal Jamu Indonesia*, **10**, 93(2025), https://doi.org/10.56108/jji.v10i2.400
20. I.M. Cahyani, T.T. Tanzaq, R.D. Agustina, and K.E. Setiawati, *Jurnal Jamu Indonesia*, **10**, 121(2025), https://doi.org/10.56108/jji.v10i2.403

[RJC-9258/2025]